N64-20656

30

CASE FILE COPY

BOEING

APPLICATION OF RESIDUAL FEEDBACK TO

LUNAR ORBITER RESIDUAL ANALYSIS

(D2-100818-1)

SEATTLE, WASHINGTON

NASA CR-66738

APPLICATION OF RESIDUAL FEEDBACK TO LUNAR ORBITER RESIDUAL ANALYSIS

(D2-100818-1)

By P. E. Hong

and P. B. Liebelt

Prepared under Contract No. NAS1-7954 by
THE BOEING COMPANY
Seattle, Wash.

for

NATIONAL AERONAUTICS AND SPACE ADMINISTRATION

THE BOEING COMPANY

CODE IDENT. NO. 81205

DOCUMENT NO. D2-100818-1

TITLE: Application of Residual Feedback to Lunar Orbit Residual Analysis - Final Report

MODEL ______ CONTRACT NO. NAS 1-7954

ISSUE NO.	ISSUED TO

SEE DISTRIBUTION LIMITATIONS PAGE

PREPARED BY P.E. Hong P. B. Liebelt — P. E. Hong, P. B. Liebelt — Sept 25, 1968

SUPERVISED BY P. B. Liebelt — P. B. Liebelt — Oct 22, 1968

APPROVED BY J. A. Retka — J. A. Retka — Oct 22, 1968

APPROVED BY J. C. Graves — J. C. Graves — Oct 23, 1968

APPROVED BY ______

2-5145

U3 4287 9000 REV. 7/64

ACTIVE SHEET RECORD

SHEET NUMBER	REV LTR	ADDED SHEETS SHEET NUMBER	REV LTR	ADDED SHEETS SHEET NUMBER	REV LTR	SHEET NUMBER	REV LTR	ADDED SHEETS SHEET NUMBER	REV LTR	ADDED SHEETS SHEET NUMBER	REV LTR
i											
ii											
iii											
iv											
v											
vi											
vii											
viii											
1											
2											
3											
4											
5											
6											
7											
8											
9											
10											
11											
12											
13											
14											
15											
16											
17											
18											
19											
20											
21											
22											
23											
24											
25											

REVISIONS			
LTR	DESCRIPTION	DATE	APPROVAL

LIMITATIONS

DDC DOES NOT APPLY

This document is controlled by 2-7837

All revisions to this document shall be approved by the above noted organization prior to release.

ABSTRACT

Orbit determination in the presence of mathematical model errors produce statistics whibh are highly unrealistic. This has been definitely shown in the Lunar Orbiter data for the orbital phase in which the standard deviations on the spacecraft state vector are much too optimistic or smaller than is physically possible. A technique is described which uses feedback from the measurement residual space to the state estimate space in order to force the covariance matrix of state to be compatible with the actual measurement residuals.

KEY WORDS

Lunar Orbiter

Orbit Determination

Tracking Data

Residual Feedback

Statistics

USE FOR TYPEWRITTEN MATERIAL ONLY

TABLE OF CONTENTS

NOMENCLATURE

Symbol	Meaning
B_i	Sensitivity of measurement with respect to state at $t = t_i$, $\frac{\partial \underline{\theta}_i}{\partial \underline{X}(t_i)}$, see Equation 5.
C_i	Covariance matrix at $t_i = E((\underline{X}-\hat{\underline{X}})(\underline{X}-\hat{\underline{X}})^T)$
fV	arbitrary noise level (see eqn. 8)
I	Identity matrix
K	Kalman gain factor (see eqns. 9 & 14)
m	number of measured values
$\underline{p}$	position vector
$S(t_i, t_o)$	Transition matrix from t_o to t_i of linearized system (see eqn. 7)
t	time
$\underline{u}$	physical constants vector
u_i	noise associated with measurement, θ, at t_i
U_i	covariance of measurement noise $= E(u_i u_i^T)$
$\underline{v}$	velocity vector
$\underline{w}_i$	noise or random perturbation associated with state, $\underline{X}$, at t_i
W_i	covariance of state noise $= E(w_i w_i^T)$, also model error (see eqn. 10)
$\underline{X}(t)$	state vector composed of $(\underline{p}, \underline{v}, \underline{u})$ at time t
θ_i	measurement or data value at t_i
$\phi(t_i, t_o)$	transition matrix of state, $\underline{X}$, from t_o to t_i (see eqn. 6)
$\overline{\Delta R_i^2}$	mean square residual of i^{th} time point (see eqn. 8)

Auxiliary Notation	Meaning
E ( )	expected value of ( )
$(\ )_{cs}$	value expressed in cartesian selenocentric ~~true~~ of date
$(\ )_{DCH}$	value expressed in downrange-crossrange-attitude system
$(\ )_{Kepler}$	value expressed in Kepler elements, selenographic of date
$(\ )_i$	value at $t = t_i$
$(\ )_o$	a priori value (except for t, viz., t_o, which means epoch)
$(\ )_R$	reference trajectory value
$(\ )^T$	matrix transpose
$(\ )^{-1}$	matrix inverse
$(\hat{\ })$	optimal estimate
$(\underline{\ })$	column vector
$\Delta(\ )$	difference
$\delta(\ )$	variation

USE FOR TYPEWRITTEN MATERIAL ONLY

1.0 SUMMARY

1.1 Residual Feedback

The primary purpose of the Lunar Orbiter mission was to photograph selected areas of the lunar surface. Essential to this task was the accurate determination of the spacecraft trajectory using tracking data from the DSIF network. In any orbit determination process, success is gauged by (1) how small are the measurement residuals (observed minus predicted values) over the entire data span, and (2) how well do the estimated uncertainties match actual state dispersions (where comparative states are determined by independent methods).

The orbit determination process used in the Lunar Orbiter flight operations was based upon an a-priori weighted least squares concept. An iterative process converged upon values of the dynamical state and selected physical constants such that the mean square residual was minimized. However, because of deficiencies in the mathematical model, the residuals were relatively large in some areas. Unfortunately, the large residuals, which indicate a poorly determined state, occurred quite frequently in the periapsis region of the orbit where most of the photographs were taken. The problem was further complicated because the OD process did not reflect the model deficiency into the state covariance, hence the statistics indicated that the converged state was precisely known.

To correct these difficulties, it is necessary to incorporate the measurement residuals into the state and covariance estimation. The additional advantage of point-by-point processing instead of batch processing used by weighted least squares suggests the use of a Kalman filter. The Kalman form computes the state correction of each point by combining the previous optimal estimate with the product of a "gain factor" and the measurement residual. The correction to the covariance matrix is achieved by feeding back an average residual correction with the gain factor.

A requirement of the Kalman estimator is an accurate reference trajectory. This is provided by the standard OD method.

Once the mean square residual is minimized the trajectory represents the best fit with the existing physical model. The resultant measurement residuals reflect model errors, or random state noise. The state and covariance correction obtained by the Kalman estimator with feedback thus provide an explicit indicator of the unknown model error.

1.2 Results

Changes to the standard ODP were made to incorporate the Kalman filter and residual feedback options. Auxiliary output was provided to express the feedback results in various coordinate systems. In an attempt to establish the effects of model error, a number of factors were investigated, among these were the data arc length, lunar gravitational model, solve-for parameters, and orbit orientation with respect to both the moon and observer. The latest available lunar models, triaxial (2nd order), LRC 11/11 (4th order), and LRC 7/28B (7th order), were used along with data from two Lunar Orbiter missions (3 and 5)

1.2 (Continued)

It was found that the state vector uncertainties, as computed by feedback, were relatively insensitive to the lunar model for data arc lengths of one to three orbits. Doppler residuals did not exceed 2 or 3 hz. with position uncertainties about $\frac{1}{2}$ km. However, for long data arc lengths (2 to 4 days), residuals of 50 to 200 hz. were common with position uncertainties of 20 km. Although the magnitude of the residuals and dispersions was surprising, the fact that they increase with data span is logical since effects due to any existing model errors would be amplified with time. The unusually large residuals over extended periods of time reflects upon the poor knowledge of the lunar gravitational model, emphasizing the need for further study in this area. It should be noted that as the data arc length and average residual increased, the state dispersions computed by the standard weighted least squares ODP actually decreased, which indicated their inadequacy in the presence of model errors.

An examination of the time history of corrections to the reference trajectory and state covariance shows no consistent pattern from one orbit to the next for multiple orbit data arcs. However, for single orbit arcs there is a discernable pattern in the variation of both the Kepler elements and the down-cross-up components for successive orbits. All elements contain short period oscillations of varying frequency. No perturbational source has yet been established for these variations.

In all the statistics examined, regardless of data arc length, gravity model, etc., the dominant uncertainties have been in the size of the orbit and location of the spacecraft along the orbit. Dispersions in all the orientation angles have been small (10^{-5} to 10^{-3} degrees) compared with uncertainties in semi-major axis (.1 to 20 km), eccentricity (10^{-4} to 10^{-2}), and time from periapsis (.1 to 20 seconds). Of particular significance to post flight photo analysis is the large down-track dispersion of .1 to 20 km, especially near perilune.

Photo evaluation studies using at least two independent missions passing over the same area and photographing a given crater have shown 2 km position discrepancies. As far as can be determined, these position errors are due primarily to model effects, which in turn should be evident in the ODP statistics (with feedback). Yet, the position uncertainties computed with feedback, under the same conditions as those in the photo evaluation studies are only .1 km. Although this would seem to indicate a deficiency in the residual feedback technique, the statistics are actually consistent with the doppler residuals. The problem lies with the non-observability of model errors in short data arcs (1 to 3 orbits).

The problem of obtaining meaningful statistics for short arcs is similar to trying to use a straight line as a model to fit parabolic data (see figure below). The uncertainties computed by the standard ODP vary inversely with the number of observations, which would say that long arcs have less error, regardless of data fit.

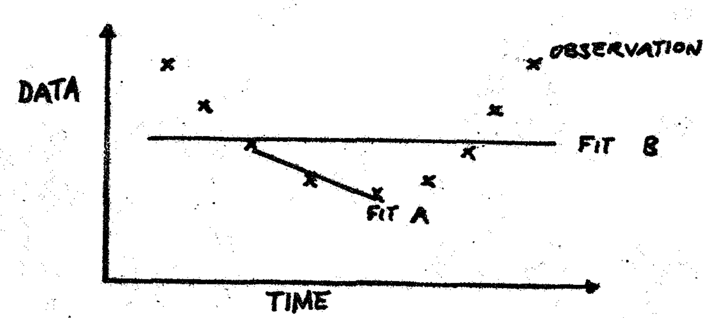

1.2 (Continued)

For short arcs (A) the linear fit is adequate and one would not expect to observe significant residuals. Thus, using residual feedback, the uncertainties due to model errors would hardly be observable. For long arcs (B) the straight line is a poor approximation to the data, the residuals become large, as do the uncertainties with feedback, and model error is clearly in evidence. It is apparent that long data arcs are necessary to provide "global" statistics for a given physical model, and successive short data arcs are useful for analysis of localized model errors.

1.3 Conclusions

The use of residual feedback to correct the state vector and covariance is successful in that the corrections do reflect the pattern of doppler residuals. However, there is a strong dependency of residuals not only on the model used, but also on the data arc length (which determines the extent of model error propagation and computational observability), on the number and type of solve-for parameters (which determine what parameter sources are available for distribution of the errors), and finally on the particular orbit and lunar region encompassed by the data arc (which affect the physical observability of the error). For these reasons, it is clear that the method of residual feedback provides statistics selective to the model of the process. Because the current lunar gravitational models are very poor, corresponding large statistics (greater than the emperical errors of the photo analysis) occur with long data arcs. Short data arcs produce small statistics and cannot provide global statistics. Hence, until basic improvements are made in the gravitational model, realistic global statistics will not be available. Thus, the feedback technique is not attractive for photo site analysis with the available gravitational models.

1.4 Recommendations

Based upon the results and conclusions,of applying residual feedback to Lunar Orbiter data, the following measures are recommended.

- Obtain better gravity coefficients either by solving for very high order models, or by determining coefficients of a different expansion series than (Legendre) spherical harmonics.

- Use long data arcs with residual feedback to determine the adequacy of improved physical models and to obtain meaningful statistics which relate one lunar area to another.

- Investigate the possible existence of mass concentrations on or near the lunar surface and include these in the physical model. One possible method of analysis is to compute a residual acceleration vector, that is the difference between the actual spacecraft acceleration and the total acceleration produced by the model. The actual acceleration may be obtained by numerical differentiations of the spacecraft velocity as corrected by residual feedback. An alternate method of computing the

1.4 (Continued)

residual acceleration is to use the standard Lagrange orbital rate equations and solve for the (downrange-crossrange-altitude) perturbing acceleration based upon the corrected osculating conic. Once the residual acceleration is known, it remains only to determine whether the vector points consistently to (or from) a lunar region. Solutions from single orbit data arcs which cover the entire lunar surface should provide sufficient information to determine the extent of mass concentrations.

USE FOR TYPEWRITTEN MATERIAL ONLY

2.0 INTRODUCTION

The development of models to simulate the real world is a standard procedure used to solve complex technical problems. In addition to the deterministic solution, it is desirable to know the accuracy of the model in terms of its effect on the solution reliability.

For Lunar Orbiter flight path control, the basic problem was to compute the dynamical state of the spacecraft at some given time. A measure of the state accuracy could be found by comparing the theoretical doppler shift of the computed trajectory with the signal actually received by the tracking station(s). The standard orbit determination process converged upon a solution for the state such that the difference in doppler, or residuals, was minimized. However, it was found that the primary contribution to the residuals was a model deficiency and not measurement error, computational limitations, and mechanical or hardware problems, although all of the latter contributions were by no means negligible.

Since the residuals are directly affected by model errors, then a good way to improve the estimation of state dispersions is to transform the residuals back into state space. As the mechanism for residual feedback, it is proposed that the Kalman filter be used. The following sections discuss the application of a Kalman estimator with residual feedback.

2.1 The Basic Orbit Determination Problem

Orbit Determination is the process of converting a given set of physical measurements into a set of constants which define the dynamical state of the orbiting particle at some given time. The measurements could consist of sets of range, azimuth, elevation, range rate, or doppler data obtained from tracking sites while observing the particle in its orbit. The set of constants being determined usually consists of position, velocity, tracking station locations and the physical constants.

The mathematical definition of the orbit determination problem is given as follows. Given a set $\underline{\theta}$ $(\theta_1, \theta_2, \ldots, \theta_m)$ of measured values such as doppler counts, estimate state vector $\underline{x}$ comprised of position $\underline{p}$, velocity $\underline{v}$, and physical constants $\underline{u}$ such that the diagonal elements of the mean error matrix $C = E(\hat{\underline{x}} - \underline{x})(\hat{\underline{x}} - \underline{x})^T$ are minimum. $\hat{\underline{x}}$ is the average state, or $E(x)$. In case a priori values $\underline{x}_o$ of $\underline{x}$ and its associated mean square error matrix $C_o = E(\hat{\underline{x}}_o - \underline{x})(\hat{\underline{x}}_o - x)^T$ are known, either the so called a priori weighted least squares or the Kalman form of optimal estimation may be employed [1].*

The mathematical representation of an orbiting satellite has the non-linear form

$$\dot{\underline{x}} = \frac{d}{dt}\begin{pmatrix} \underline{p} \\ \underline{v} \\ \underline{u} \end{pmatrix} = \begin{pmatrix} \underline{v} \\ \underline{f}\,(\underline{x},\underline{u}) \\ o \end{pmatrix} + \underline{w}(t) \qquad (1)$$

for computation of the state vector, and the form

$$\underline{\theta}_i = \theta(\underline{x}(t_i)) + u_i \qquad (2)$$

---

* [ ] Refers to reference number.

USE FOR TYPEWRITTEN MATERIAL ONLY

U3 4802 1434 REV 9-65

2.1 (Continued)

for the measurement process where u_i represents the noise of the measurement and $\underline{w}_i$ represents a noise or random perturbation of the state at time t_i. Usually the state perturbation process $\underline{w}(t)$ is considered negligible in orbit determination problems. However, when state noise is included, then the following assumptions are usually made concerning the random process w_i and u_i:

$$E\,(\underline{w}_i\ \underline{w}_i^T) = W_i$$

$$E\,(\underline{w}_i\ \underline{w}_j^T) = 0 \qquad i \neq j$$

$$E\,(u_i^2) = U_i$$

$$E\,(u_i\ u_j) = 0 \qquad i \neq j$$

$$E\,(u_i\ \underline{w}_j^T) = 0 \tag{3}$$

In order to apply optimal-estimation procedures in a practical fashion, Equations (1) and (2) must be linearized about some reference state vector:

$$\frac{d}{dt}\,(\delta\underline{x}) = \frac{d}{dt}\begin{bmatrix}\delta\underline{p}\\ \delta\underline{v}\\ \delta\underline{u}\end{bmatrix} = \begin{bmatrix}0 & I & 0\\ F & 0 & G\\ 0 & 0 & 0\end{bmatrix}\begin{bmatrix}\delta\underline{p}\\ \delta\underline{v}\\ \delta\underline{u}\end{bmatrix} \tag{4}$$

$$\Delta\theta_i \cong \delta\theta_i = B_i\ \delta\underline{x}_i \tag{5}$$

where

$$F = \frac{\partial\underline{f}}{\partial\underline{p}},\quad G = \frac{\partial\underline{f}}{\partial\underline{p}},\ \text{and}\ B_i = \frac{\partial\theta_i}{\partial\underline{x}(t_i)}$$

The formal solution to equation (4) can be written as follows:

$$\delta\underline{x}(t) = \begin{bmatrix} S(t,t_o) & \displaystyle\int_{t_o}^{t} S(t,s)G(s)ds \\ 0 & I \end{bmatrix} \delta\underline{x}(t_o) = \phi\,(t,t_o)\ \delta\underline{x}(t_o) \tag{6}$$

where $S(t,t_o)$ is the state transition matrix of the linear system

$$\dot{S}(t,t_o) = F(t)\ S(t,t_o)$$
$$S(t_o,t_o) = I \tag{7}$$

LUNAR ORBITER DOPPLER RESIDUALS FIGURE 1

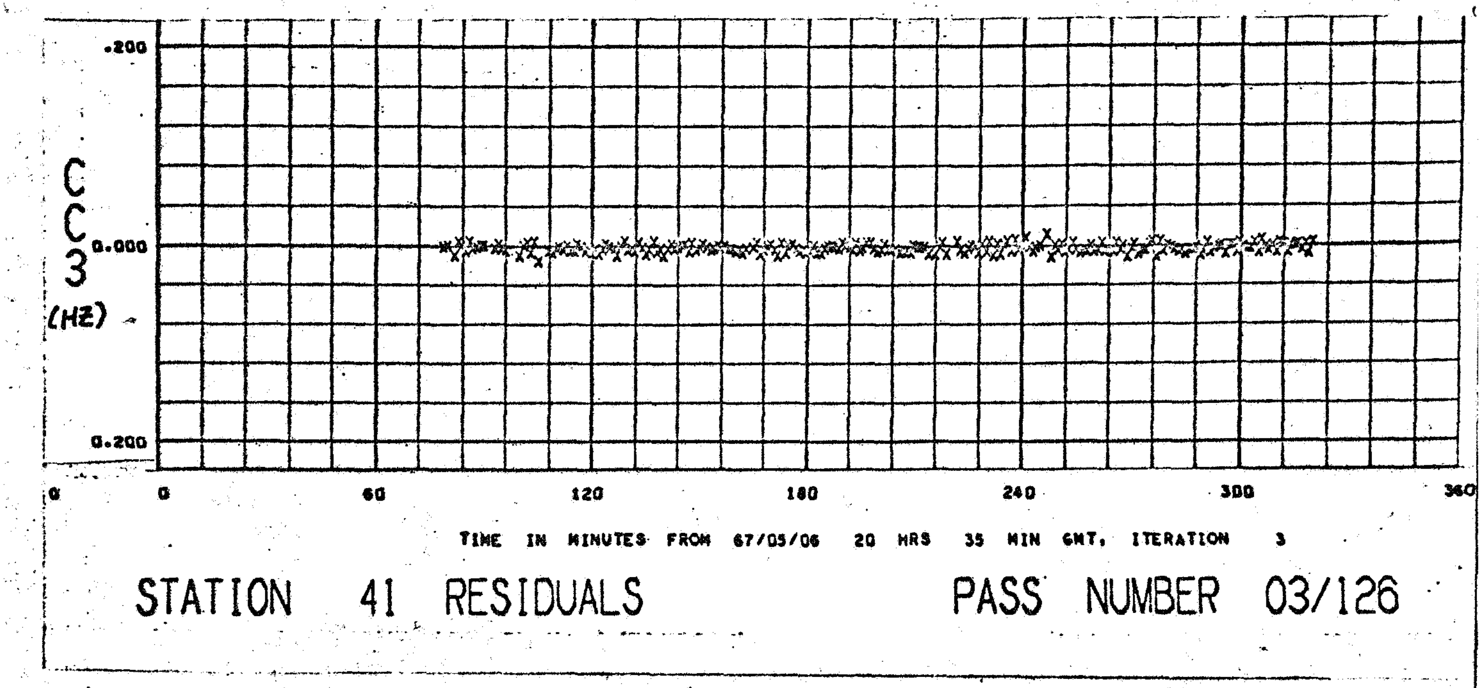

TRANSLUNAR (FIG. 1a)

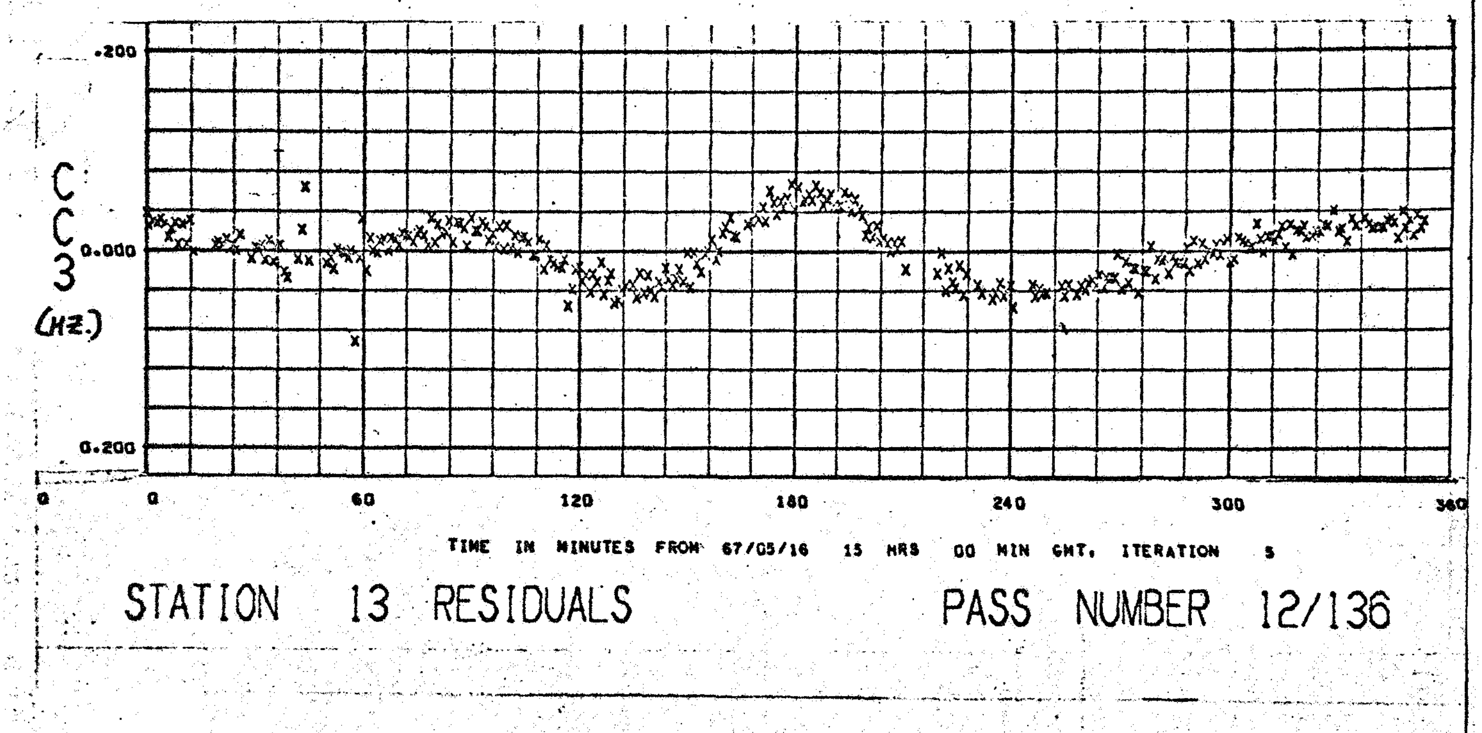

LUNAR ORBIT (FIG. 1b)

2.1 (Continued)

Using this linear model to describe deviations from a trial solution to the orbit determination problem, optimal estimation theory [1] is applied in an iterative or recursive manner to obtain a definitive orbit of the observed particle or point mass. The forms available for optimal estimation will be discussed in detail in the following sections.

2.2 The Model Error Problem

Any description of the real world by mathematical equations must contain some approximation. The inadequacies of the resulting approximations are known as "modeling errors". These errors may produce serious deficiencies with their subsequent use. Moreover, they cannot be eliminated or made negligible in all cases. For example, the Lunar Orbiter project furnished a prime example of such a situation. It now appears that the mathematical description of the physics of an orbiting vehicle about the moon is not known within the possible accuracy derived from measurement data. In summary, mathematical model errors are always present in any quantitative description of a physical process and, furthermore, they may be significant despite all efforts to obtain better approximations.

The orbit determination process of obtaining the ephemeris of a spacecraft from measurement data furnished via a tracking network is also subject to modeling errors. With respect to the Lunar Orbiter project, it now appears that the lunar gravitational field is very complex and will require intensive investigation into postulating and testing an adequate potential model.

Figure 1 is a typical example of doppler residuals (difference between expected and actual doppler shift) due to model errors. During the translunar phase (Figure 1a), the residuals are small and random. In lunar orbit, however, it can be seen that the residuals are not due to random noise but rather due to a consistent perturbation. The harmonic model used was the best available fourth order model generated by NASA at this time.

The presence of known model errors has several adverse effects upon the results of orbit determination. First and foremost, the solution obtained is corrupted in accuracy and the model errors may even cause divergence of the orbit determination process. Also, the corresponding statistics of the selection may be too optimistic by several orders of magnitude. As an example of this later phenomenon, one orbit determination was made using three orbits of doppler data during Lunar Orbiter Mission 3. Another determination was made using data from Mission 5. A crater which was common to photographs in both missions was chosen as a checkpoint. The orbit determinations when combined with spacecraft attitude and time information give the site location as follows:

Mission		Longitude (deg)	Latitude (deg)
3		358.885	0.491
5		358.911	0.435
	Difference (km)	0.79	1.70
	RSS Error	1.87 km	

USE FOR TYPEWRITTEN MATERIAL ONLY

2.2 (Continued)

The corresponding statistics of the two orbit determinations were as follows:

Mission	RSS Position error
3	0.12 Km
5	0.10 Km

From comparison of position errors, it is obvious that the theoretical error statistics from the orbit determination processes are erroneous and much too optimistic.

It must be emphasized, however, that the orbit determination statistics are the theoretically obtainable accuracy levels in the absence of model errors. In other words, if the mathematical model were known perfectly, than the orbit determination process is capable of determining the position of a lunar satellite with incredible precision using the available doppler data from the DSIF tracking network.

2.3 Compensation For Model Errors

The recognition that model errors do exist in the orbit determination process is of fundamental importance. For then one can postulate the existence of such errors and compensate for their absence. It should be pointed out that if model errors are present, they will eventually manifest themselves in an unexplained increase in the average measurement residual.

There are three common methods to overcome model errors. The first is to limit the tracking-data arc length so that model errors are of the same magnitude as the noise in the data. This method is reported in Reference [2] . The second method is analytic in nature in which one postulates the existence of specific model errors and computes the resulting theoretical effects of each of the assumed model error sources. Reference [3] furnishes an example of this type of compensation. The third method, the feedback method, uses an empirical correction to the optimal estimate in use to make the statistics of the estimate-space compatible with the observed statistics of the measurement-space. We will use the feedback method since it limits the data in a rational, analytical, and automatic fashion.

2.4 The Principle of Feedback Compensation

The fundamental idea beneath the concept of residual feedback is the realization that the performance of an estimator, including the optimal estimate, can be determined from an examination of the residuals. This is accomplished by comparing the calculated mean square residual against some expected level of measurement noise. If the mean square residual is consistently larger or is growing larger than the noise level, it must be concluded that an unknown model error is present in the mathematical representation of the observable. The origin of the model error may be in the measurement space or the state space or in both. With multiple data sources, it is at least possible in theory to detect measurement biases and correct the model to account for these biases. Without multiple data sources it is impossible to decide upon the origin of the model error.

USE FOR TYPEWRITTEN MATERIAL ONLY

2.4 (Continued)

Assuming that there is adequate compensation for all measurement biases and that the mean square residual is either already too large or is growing rapidly, it must be concluded that an unknown model error exists in the state space. With respect to the Lunar Orbiter missions, this could mean that there is an ill-described force acting on the spacecraft such as various high order harmonic perturbations. As a matter of fact, large residuals are in evidence in the Lunar Orbiter orbit determination studies [4] performed to date. Furthermore, the translunar portion of flight clearly indicates that there are no unknown model errors or biases in the measurement space and the unexplained level of mean square error must be due to a model error in the state space. The suggested computation of the mean square residual is as follows:

$$\overline{\Delta R}_i^{\,2} = \text{Max}\left[\,0, \left(\frac{1}{j} \sum_{k=i-j}^{i} \Delta\,\theta_k^{\,2}\right) - fV\,\right] \tag{8}$$

The integer j and the quantity fV may be determined by prior experience. Note that whenever the mean square residual is less than the noise level, fV, the quantity $\overline{\Delta R}_i^2$ is zero.

Having detected the presence of an unexpected level of mean square residual error, there remains the problem of compensation for the effect. Many investigators artifically use unreasonably large values of noise level statistics in the equation of the optimal estimation. This latter procedure only delays the problem and cannot adequately offset the effects of model errors in the state space. Rather, one must acknowledge the existence of model errors and modify the behaviour of the optimal estimate to compensate for the detected error.

The computation of the magnitude of the assumed state model error poses a difficult problem. One must specify a transformation from the residual space to the state space. An examination of the optimal estimation leads one to conclude that the Kalman gain matrix *, K, from the equation

$$\hat{\underline{x}} = \hat{\underline{x}}_o + K\,\Delta\underline{\theta}_i \tag{9}$$

is a logical choice for the transformation since

$$\frac{\partial\,\underline{x}}{\partial\theta_i} \cong \frac{\Delta\hat{\underline{x}}}{\Delta\theta_i} = \frac{\hat{\underline{x}}-\hat{\underline{x}}_o}{\Delta\,\theta_i} = K$$

The specific method suggested to map the mean square residual $\overline{\Delta R}_i^{\,2}$ back to the state space has the form

$$W_i = K \quad \overline{\Delta R}_i^{\,2} \quad K^T \tag{10}$$

The suggested procedure of mapping the mean square residual back to the state space does violate one assumption used in the derivation of the optimal

* The algorithm required to compute K is given in latter sections.

USE FOR TYPEWRITTEN MATERIAL ONLY

2.4 (continued)

estimator. A model error in the state space is usually assumed to be uncorrelated in time--at least, this assumption is used in the following material. However, the model errors in the state space of the Lunar Orbiter would tend to be correlated in time, at least over a period of a few minutes. This defect can be eliminated by choosing data at infrequent time intervals--that is, a time interval larger than the period of significant time correlation.

3.0 SPECIFICATION OF THE FEEDBACK PRINCIPLE

3.1 The Weighted Least Square Estimator

The current orbit determination program ODPL used for the Lunar Orbiter project uses the following a priori weighted least square form for a fixed epoch of time:

$$\left.\begin{aligned}
\hat{\underline{x}}(t_o) &= \hat{\underline{x}}_o(t_o) + \delta \hat{\underline{x}}(t_o) \\
\hat{\theta}_i &= \theta(\hat{\underline{x}}(t_i)) \\
\Delta\theta_i &= \hat{\theta}_i - \theta_i \cong B_i \phi(t_i, t_o) \delta \hat{\underline{x}}(t_o) \\
\delta \hat{\underline{x}}(t_o) &= C\left[C_o^{-1}(\hat{\underline{x}}_o(t_o) - \hat{\underline{x}}(t_o)) + \sum_{i=1}^{m} B_i^T \phi_i U_i^{-1} \Delta\theta_i\right] \\
C &= \left[C_o^{-1} + \sum_{i=1}^{m} B_i^T \phi_i^T U_i^{-1} \phi_i B_i\right]^{-1}
\end{aligned}\right\} \quad (11)$$

where $\hat{\underline{x}}_o$ and C_o are the a priori, or previous optimal, estimate and covariance matrix, respectively. $\phi_i = \phi(t_i,t_o)$, B_i, and U_i are defined in equations 6, 5, and 3, respectively. The dependence of $\hat{\underline{x}}_o$, C, B_i, and $\phi(t_i, t_o)$ on one another requires iterating until the mean square measurement residual reaches a stationary value. Assuming the iteration process converges, then the resultant trajectory is used as a reference for applying the Kalman estimator, which is described in the following sections. A complete operational description of the ODPL program with residual feedback can be found in Reference [5] .

3.2 Kalman Floating Epoch Estimator

The computational algorithm for the floating epoch form with or without feedback is as follows:

An initial estimate of the (optimal) state, $\hat{\underline{x}}(t_i)$, is computed using the optimal estimate and correction of the previous time point.

$$\begin{aligned}
\hat{\underline{x}}(t_i) &= \hat{\underline{x}}(t_{i-1}) + \int_{t_{i-1}}^{t_i} \dot{\underline{x}}(\hat{x}(t_{i-1}))ds \quad \text{if } \delta\hat{x}(t_{i-1}) > \epsilon \\
\hat{\underline{x}}(t_i) &= \underline{x}_R(t_i) + S(t_i,t_{i-1}) \delta \hat{\underline{x}}(t_{i-1}) \quad \text{if } \delta\hat{x}(t_{i-1}) \le \epsilon
\end{aligned} \quad (12)$$

USE FOR TYPEWRITTEN MATERIAL ONLY

3.2 (Continued)

where ϵ is an arbitrarily small parameter to be chosen by the user. $\underline{x}_R(t)$ refers to the reference trajectory. Next, the measurement residual, $\Delta\theta_i$, and an initial correction to the state, $\delta\hat{\underline{x}}(t_i)$, are computed.

$$\left.\begin{aligned} \Delta\theta_i &= \theta(\hat{\underline{x}}(t_i)) - \theta_i \\ \delta\hat{\underline{x}}(t_i) &= \hat{\underline{x}}(t_i) - \underline{x}_R(t_i) \end{aligned}\right\} \quad (13)$$

Using the covariance of the previous time point, C_{i-1}, an initial value of the covariance, C_i, and Kalman gain factor, K, are computed.

$$\left.\begin{aligned} C_i &= S(t_i, t_{i-1})\, C_{i-1}\, S^T(t_i, t_{i-1}) \\ K &= C_i B_i (U_i + B_i{}^T C_i B_i)^{-1} \end{aligned}\right\} \quad (14)$$

Finally, the optimal correction, $\delta\hat{\underline{x}}_i$, state, $\hat{\underline{x}}_i$, and related covariance can be calculated:

$$\left.\begin{aligned} \delta\hat{\underline{x}}_i &= \delta\hat{\underline{x}}_i + K\left[\Delta\theta_i - B_i\, \delta\hat{\underline{x}}_i\right] \\ \hat{\underline{x}}_i &= \underline{x}_R(t_i) + \delta\hat{\underline{x}}_i \\ C_i &= C_i - KB_iC_i + W_i \end{aligned}\right\} \quad (15)$$

Without feedback $W_i = 0$, whereas with feedback, W_i is defined by equation (10). It is important to observe that both a measurement noise, U_i, and a state perturbation, W_i, can be accommodated with this type of estimation.

3.3 Kalman Fixed Epoch Estimator

Another variation of optimal estimation in the presence of model errors uses a fixed epoch rather than the floating form of equations (12) through (15). The basic equations, given below, combine features of the a priori weighted least squares and the floating Kalman epoch forms:

$$\left.\begin{aligned} \hat{\underline{x}}(t_i) &= \hat{\underline{x}}(t_o) + \int_{t_o}^{t_i} \dot{\underline{x}}\,(\hat{\underline{x}}_o(t_o), s)\, ds \qquad \text{if} \quad \delta\hat{\underline{x}}(t_{i-1}) > \epsilon \\ \hat{\underline{x}}\,(t_i) &= \underline{x}_R\,(t_i) + S(t_i, t_{i-1})\, \delta\hat{\underline{x}}(t_{i-1}) \qquad \text{if} \quad \delta\hat{\underline{x}}(t_{i-1}) \le \epsilon \end{aligned}\right\} \quad (16)$$

$$\left.\begin{aligned} \Delta\theta_i &= \theta(\hat{\underline{x}}(t_i)) - \theta_i \\ \delta\underline{x}(t_o) &= \hat{\underline{x}}(t_o) - \underline{x}_R\,(t_o) \end{aligned}\right\} \quad (17)$$

3.3 (Continued)

$$
\left.
\begin{aligned}
K &= C_o \, \phi^T (t_1, t_o) \, B_1^T \left[U_1 + B_1 \phi (t_1, t_o) \, C_o \, \phi^T (t_1, t_o) B_1^T \right]^{-1} \\
\delta \hat{\underline{x}}(t_o) &= \delta \hat{\underline{x}}(t_o) + K \left[\Delta\theta_1 - B_1 \, \phi(t_1, t_o) \, \delta \hat{\underline{x}}(t_o) \right] \\
\hat{\underline{x}}(t_o) &= \hat{\underline{x}}(t_o) + \delta \hat{\underline{x}}(t_o) \\
C &= C_o - K B_1 \, \phi (t_1, t_o) \, C_o \\
C_o &= C + W_1 \quad .
\end{aligned}
\right\} \quad (18)
$$

3.4 Use of a Reference Trajectory

The use of an accurate reference trajectory in both the Kalman fixed and floating epoch estimators omits the need to iterate when processing data points. It also ensures the accuracy of feedback results due to linearity considerations. If the reference trajectory has been derived with the standard weighted least squares estimator, then the corresponding mean square measurement residuals have reached a stationary value. The residuals can now be said to directly reflect any model error or random state noise. The use of residual feedback and point-by-point processing with the Kalman estimator then corrects the state and covariance matrix. The corrected state and statistics should be improved with respect to the data fit, and when compared to the reference trajectory, the effects of model uncertainties are explicitly illustrated.

4.0 APPLICATIONS OF THE THEORY

4.1 Coordinate Systems

It is often more descriptive to express the state and state deviations in coordinate systems other than the cartesian selenocentric true of date system in which the ODP operates. Two useful, of date, systems are Keplerian orbital elements and cartesian downrange-crossrange-up (DCH) components. The state vectors involve standard point transformations [6] ; however, the state deviations from a reference solution and state covariance utilize a different means of transformation.

The transformation from cartesian selenocentric (cs) to Kepler selenographic coordinates involve computing a Jacobian matrix [6] ,

$$Q(t) = \frac{\partial \underline{x}_{Kepler}}{\partial \underline{x}_{cs}}$$

The Kepler state deviations and covariance are then given by

$$\delta \underline{x}_{Kepler} = Q \, \delta \underline{x}_{cs}$$

$$C_{Kepler} = Q \; C_{cs} \; Q^T$$

Conversion to the DCH system requires the matrix

$$R(t) = \begin{bmatrix} \dfrac{\underline{p}}{|\underline{p}|} \\ \\ \dfrac{(\underline{p} \times \underline{v}) \times \underline{p}}{|(\underline{p} \times \underline{v}) \times \underline{p}|} \\ \\ \dfrac{\underline{p} \times \underline{v}}{|\underline{p} \times \underline{v}|} \end{bmatrix}$$

4.1 (continued)

The state deviations and covariance are given by

$$\delta \underline{x}_{DCH} = \begin{bmatrix} R & O \\ O & R \end{bmatrix} \delta \underline{x}_{cs}$$

$$C_{DCH} = \begin{bmatrix} R & O \\ O & R \end{bmatrix} C_{cs} \begin{bmatrix} R^T & O \\ O & R^T \end{bmatrix}$$

In addition to the ODP modifications which incorporated the Kalman filter and residual feedback option, the expression of all feedback results was expressed in the three coordinate systems: cartesian selenocentric, Kepler selenographic, and cartesian downrange-crossrange-altitude.

USE FOR TYPEWRITTEN MATERIAL ONLY

4.2 Statistics Improvement

Statistics which approach observed dispersions can be obtained by using the Kalman estimator with residual feedback. However, the statistics reflect the residual pattern which in turn is governed by such variables as type of solve-for parameters, data arc length, data type, and orbit geometry with respect to the observer.

Care must be taken that the statistics are not artificially stimulated. For example, this would occur if the a-priori state covariance differed from the actual (as computed by feedback) by an order of magnitude. It would then require at least one orbit for the statistics to settle out. In addition, the doppler data must be relatively "clean". If a bad data point is encountered, then the statistics become distorted and several good points must be processed before the statistics return to normal.

Table 1 summarizes the RSS of position and velocity standard deviations as computed by the standard ODP statistics. The one exception is the case where fixed epoch residual feedback was employed for comparison. All statistics are evaluated near the data epoch (approximately -130 degrees true anomaly). Area D is the checkpoint location discussed in Section 2.2, that is, a crater at 359 degrees longitude, 0 degrees latitude, with an estimated dispersion of 1.9 km based on photo consistency studies. Area H is a crater located on the lunar western hemisphere at 324 degrees longitude, -4 degrees latitude, with an estimated dispersion of 1.2 km. The principal orbit parameters of Missions 3 and 5 are:

Mission	3	5
Perilune altitude* (km)	50	100
Apolune altitude* (km)	1850	1500
Period (min.)	209	191
Orbital inclination (deg.)	21	85

* Above a 1738 km mean lunar radius

The perilune of both missions was near the equator, although photography occurred on the descending node (North to South) for Mission 3 and on the ascending node for Mission 5.

It is apparent in Table 1 that the statistics are too optimistic even for the case of residual feedback. The single exception is the one orbit data arc over area H where it is suspected that the statistics are not so much an indication of model error as they are of insufficient observability, i.e., tracking data. It is also significant that as the data arc increased (cases 6, 7, 5), the average residual also increased, but the ODP uncertainties decreased.

When feedback is used in its floating epoch form, statistics are generated at every time point. It is of particular interest to examine the region near perilune where most of the Lunar Orbiter photography occurred. Table 2 summarizes the position and velocity dispersions at perilune over the stated checkpoint areas. There is a noticeable improvement in the statistics over those produced by the standard OD; however, suspected position dispersions of 1 to 2 km do not occur for the 3 orbit data arcs. This is not too surprising in light of the doppler residual size, and emphasizes the difficulty of observing model errors

Case	Average Doppler Residual (hz)	Position RSS (km)	Velocity RSS (met/sec)	Mission	Area	Data Arc (Orbits)	Solve-for
1	.37	.18	.04	5	D	3	STATE + HARMONICS
2	.54	.05	.05	3	D	3	STATE
3	.80	.08	.03	5	D	3	STATE
4	.80	.45	.25	5	D	3	STATE (WITH FEED-BACK)
5	50.	.005	.003	5	....	16	STATE
6	.21	1.85	.74	5	H	1	STATE + [illegible]
7	.22	.11	.04	5	H	3	STATE + HARMONICS
8	1.05	.05	.02	5	H	3	STATE

TABLE 1. Position, Velocity Dispersions at Epoch (from ODP)

Case	Average Doppler Residual (hz)	Position RSS (km)	Velocity RSS (met/sec)	Mission	Area	Data Arc (Orbits)	Solve-for
2	.54	.05	.08	3	D	3	STATE
3	.80	.22	.18	5	D	3	STATE
5	50.	10.34	7.8	5	D	16	STATE
6	.21	6.10	9.3	5	H	1	STATE
7	.22	.16	.12	5	H	3	STATE + HARMONICS
8	1.05	.13	.22	5	H	3	STATE

TABLE 2. Position, Velocity Dispersions at Perilune (from feedback)

USE FOR TYPEWRITTEN MATERIAL ONLY

4.2 (Continued)

in short data arcs. Unlike statistics from the weighted least squares ODP, the uncertainties computed by feedback increase as the data arc length and resultant doppler residuals increase. Again, the statistics for the one orbit data arc over area H probably reflects the lack of data more than model deficiencies.

Table 3 summarizes the standard deviations near perilune in down-cross-up state space. Throughout all the feedback runs was a consistent uncertainty in the downrange position of the spacecraft which usually overshadowed the dispersion in crossrange and altitude. It is important to note that a downrange (and crossrange) error will seriously affect the post-flight determination of photo locations.

As an example of the long term variation of position uncertainties, Figure 2 illustrates the doppler residual and the downrange-crossrange-altitude standard deviations at perilune for the second through fourteenth orbits of the mission five 16 orbit data arc. The corresponding node longitude varied from 359.1 degrees for the second orbit to 338.1 degrees for the fourteenth orbit.

Dispersions in Kepler space are summarized in Table 4. The uncertainties in spacecraft position are shown by the relatively large standard deviations in semi-major axis, eccentricity, and periapsis time. Since the spacecraft moves approximately 1.8 km/sec at perilune, an error of $\frac{1}{2}$ second in periapsis time could result in a downrange error of almost one km. Unlike the position, the orbit orientation angles appear to be well defined. The large residuals and dispersions for the 16 orbit data arc are actually outside the assumptions of linearity and may be erroneous.

When one considers the results of the 16 orbit data arc presented in Tables 1 through 4 and Figure 2, the need for an adequate lunar gravitational model is obvious. Using any of the latest sets of gravitational coefficients, and long data arcs (2 or more days), the doppler residuals are undesirable with respect to the linearity assumptions within the feedback process, and intolerable as a measure of lunar model accuracy.

4.3 Deviations From a Reference Solution

At each time point, the feedback process not only computes the state covariance, but also estimates the necessary correction to the reference trajectory in order that the residual be reduced to zero. If the reference trajectory is a converged solution of the weighted least squares ODP, then the state deviations computed by feedback are caused primarily by model deficiencies. Furthermore, if the deviations are due to model deficiencies, then there should be some consistency in doppler residuals and state deviations from one orbit to the next. Because of the fitting process, there was no consistency in results obtained for multiple orbit data arcs. However, when single orbit arcs were used, a repeatable pattern in both residuals and state deviations became evident. A disadvantage of the short arc was the presence of large uncertainties due to the relatively small amount of data available. For this reason, care should be taken in interpreting the size of the state deviations.

USE FOR TYPEWRITTEN MATERIAL ONLY

4.3 (Continued)

Figure 3 shows the time history of corrections to the reference trajectory in various parameters during the interval of 15 minutes before and after perilune for Mission 5, area H, one orbit arc, with a triaxial moon, solving for state only. It illustrates the typically large changes in orbit size as seen in the semi-major axis (3b), the small orbit orientation corrections as seen in the inclination (3c), and the large standard deviations along the orbit track (3d). All parameter variations in time resemble the doppler residuals (3a) and are consistent with the statistics experienced in section 4.2.

It is interesting to compare the behavior of standard deviations (3d) with corrections to the reference trajectory (3b and 3c). The state corrections are computed using only one measurement residual at a time whereas the state dispersions use (in this case) the RMS of 5 data points. Thus, the effect of rapidly changing residuals are much more noticeable in state corrections than in state dispersions. If a perturbing source is associated with local lunar terrain, as is often hypothesized [7] , then one would expect a slight but rapid change in doppler as the spacecraft passes over the perturbation. The resultant doppler residual will be transformed into a quick change in the state deviations from the reference trajectory.

The consistency between one orbit data arcs is illustrated in Figure 4. The downrange correction to the reference trajectory is shown as it changes with time over the data span for two cases which are separated by one orbit. The $\Omega = 325^{\circ}$ case is the same as that presented in Figure 3. It is unfortunate that tracking data is lacking near perilune for the $\Omega = 328^{\circ}$ case. The missing data would, of course, affect the results somewhat. Examination of the available downrange corrections show a consistent pattern between the two cases. There is evidently a perturbation near perilune and another, perhaps, approximately 27 minutes past perilune (76 degrees latitude). If the perturbations are attributed to surface mass concentrations, then the size of the initial perturbation, near perilune, may be misleading because of the inverse square relationship between spacecraft distance and gravitational attraction. At 27 minutes past perilune, the spacecraft altitude is 420 km whereas at perilune it is 100 km. Thus, a mass concentration near perilune will exert 16 times more force than the same mass encountered 27 minutes later. This type of analysis is needed in a much more precise fashion to determine the exact cause and location of the trajectory perturbations. Whatever their cause, it is apparent that the current physical model is not adequate.

Doppler Residual (hz)	Standard Deviations (Km) Downrange	Crossrange	Altitude	Mission	Area	Data Arc (orbits)	Solve-For
1.02	.05	.01	.001	3	D	3	STATE
2.23	.21	.05	.02	5	D	3	STATE
48.81	9.36	1.50	4.14	5	D	16	STATE
1.66	6.03	1.38	.10	5	H	1	STATE
1.54	.15	.01	.01	5	H	3	STATE + HARMONICS
1.53	.05	.06	.07	5	H	3	STATE

TABLE 3. Position Dispersions in Down-Cross-Up State Space

Semi-Major Axis	Standard Deviations Eccentricity (10^{-3})	Inclination (10^{-3} deg.)	Node Longitude (10^{-3} deg)	Argument of Perilune (10^{-3} deg)	Time from Perilune (sec)	Mission	Area	Data arc (orbits)	Solve-For
.65	.15	.01	.04	.05	.01	3	D	3	STATE
.46	.12	.08	.05	.47	.57	5	D	3	STATE
22.51	5.08	2.85	2.83	24.62	30.05	5	D	16	STATE
2.55	1.69	3.87	1.19	4.78	1.90	5	H	1	STATE
.19	.07	.05	.03	.35	42	5	H	3	STATE + HARMONICS
.46	.10	.07	.02	.53	.56	5	H	3	STATE

TABLE 4. Dispersions in Kepler Elements Near Perilune

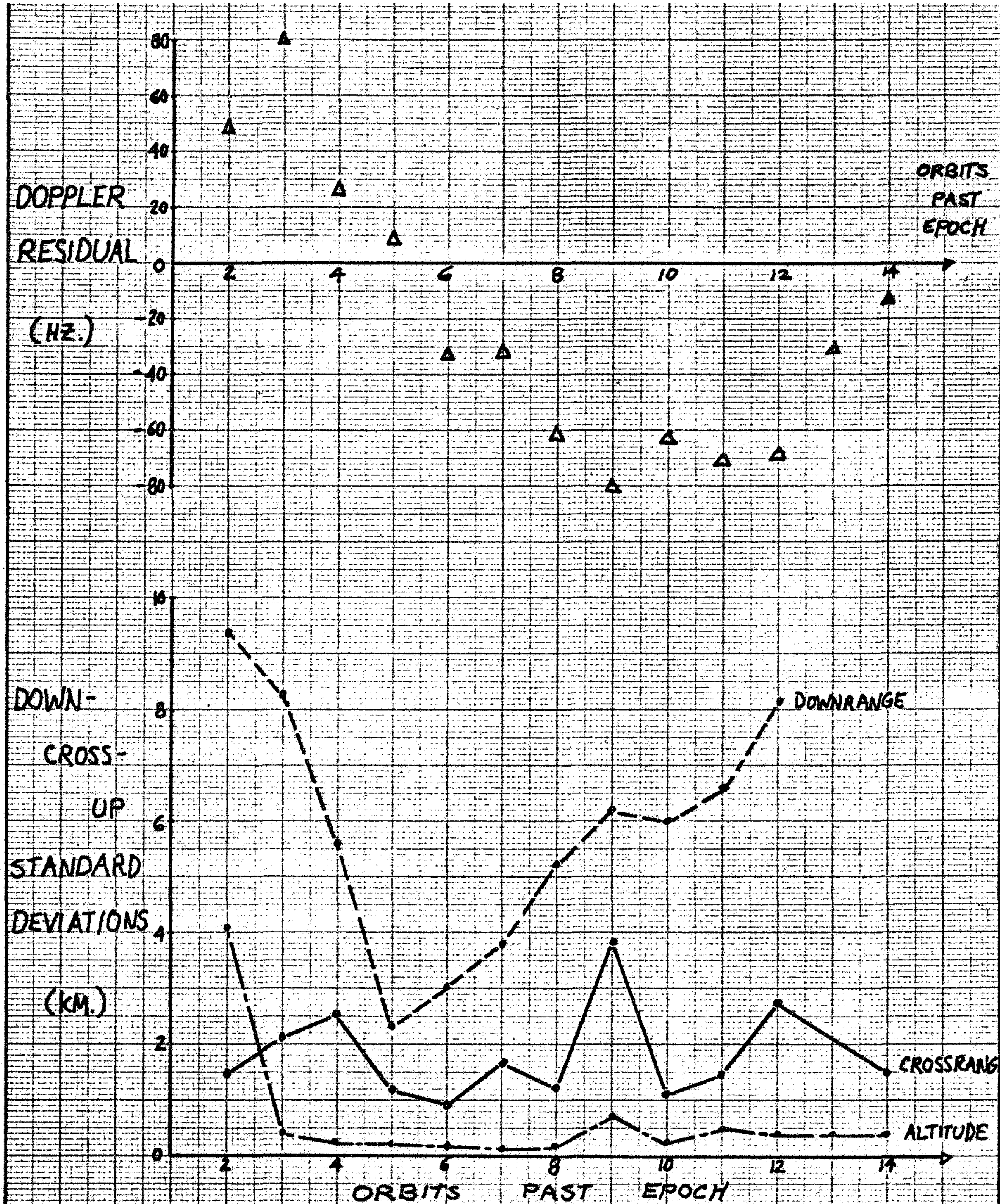

	INITIALS	DATE.	REV BY INITIAL	DATE	TITLE	MODEL
CALC	PEH	9-68			LONG TERM POSITION UNCERTAINTIES	FIG. 2
CHECK						
APPD.						
APPD.						

U3 4013 8000 REV. 1/66

REV LTR

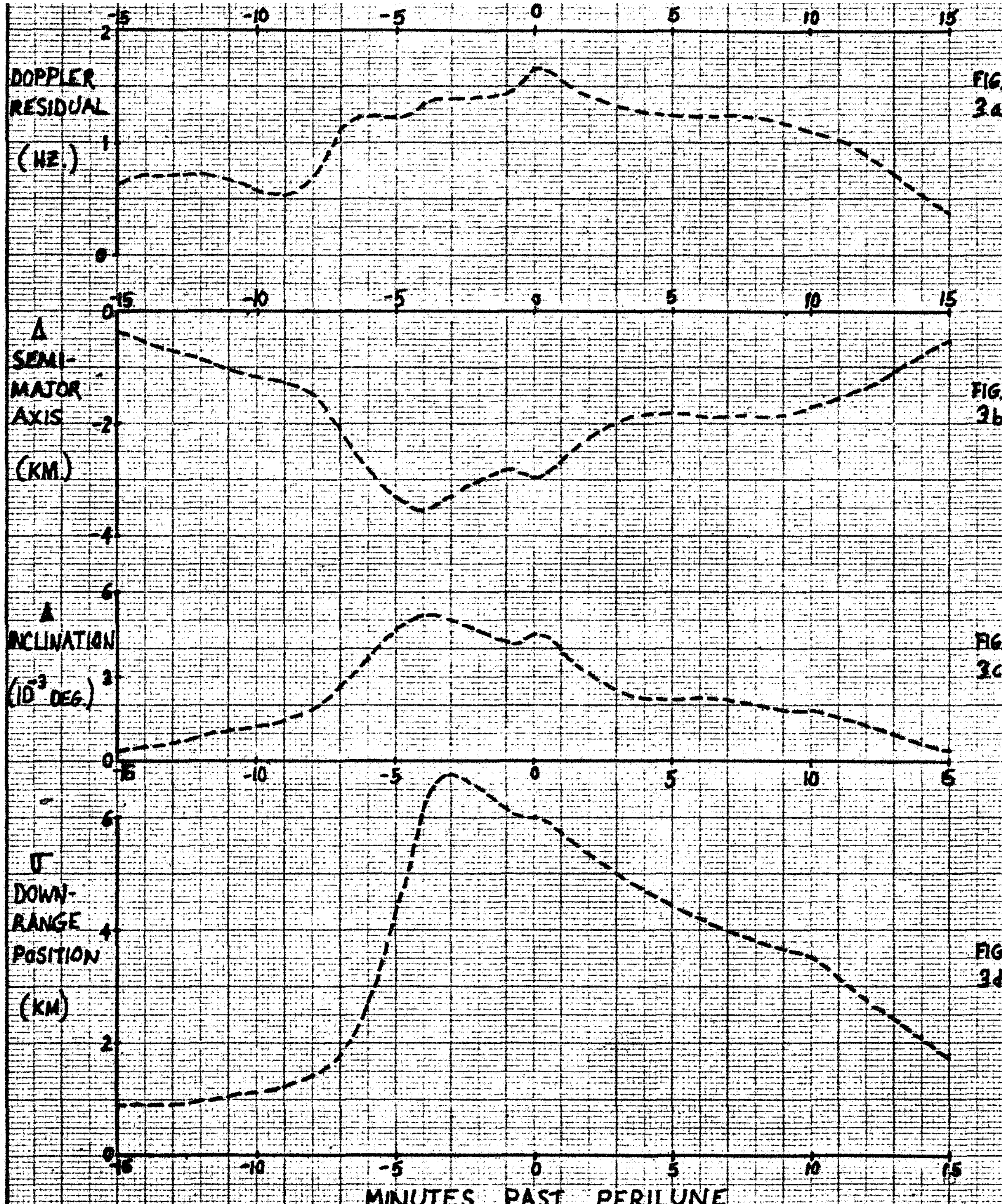

	INITIALS	DATE	REV BY INITIAL	DATE	TITLE	MODEL
CALC	PEH	9/68			DEVIATIONS FROM REFERENCE TRAJECTORY	FIG. 3
CHECK						
APPD.						
APPD.						

U3 4013 9000 REV. 1/66

REV LTR________

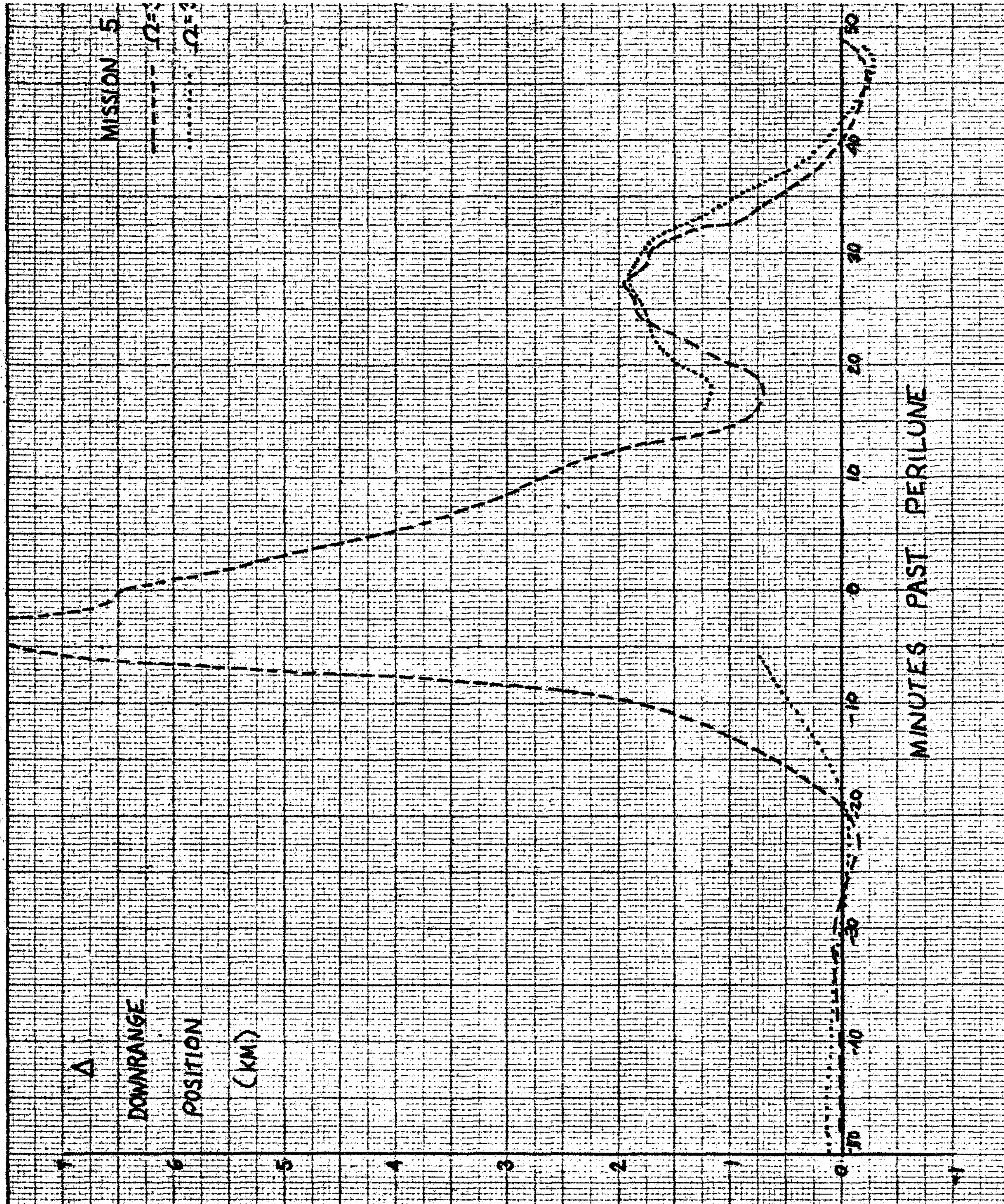

	INITIALS	DATE	REV BY INITIAL	DATE	TITLE	MODEL
CALC	PEH	9/68			DOWNRANGE CORRECTION TO REFERENCE TRAJECTORY	FIG. 4
CHECK						
APPD.						
APPD.						

U3 4013 8000 REV. 1/66

REV LTR________

5.0 References

1 An Introduction to Optimal Estimation, P. B. Liebelt; Addison-Wesley, 1967.

2 Sensitivity Analysis of Modern Optimum Filtering Methods to Unknown Model Parameters, R. Cosaert; ELDO TM-F35

3 Divergence in the Kalman Filter, F. H. Schlee, C. J. Standish, and N. F. Toda; Proceedings of AIAA/JACC Guidance and Control Conference, August 15-17, 1966.

4 Lunar Orbiter Data Analysis, J. Lorell and W. L. Sjogren; JPL TR-32-1220

5 Lunar Phase Orbit Determination Program (ODPL) Users' Guide, D. Van Zandt; TBC D2-100538-4

6 FPAC General Purpose Subprograms, F. J. Placek; TBC D2-100440-1

7 Mascons: Lunar Mass Concentrations, P. M. Muller and W. L. Sjogren; Science, August 16, 1968

USE FOR TYPEWRITTEN MATERIAL ONLY

USE FOR TYPEWRITTEN MATERIAL ONLY

DISTRIBUTION LIST

NAS1-7954

		Copies each
NASA Langley Research Center Langley Station Hampton, Virginia 23365		
Attention:	Research Program Records Unit, Mail Stop 122	1
	Raymond L. Zavasky, Mail Stop 117	1
	Wilbur L. Mayo, Mail Stop 159	1
	I. G. Recant, Mail Stop 159	1
	William H. Michael, Jr., Mail Stop 152A	1
	Albert A. Schy, Mail Stop 152B	1
NASA Ames Research Center Moffett Field, California 94035		
Attention:	Library, Stop 202-3	1
NASA Flight Research Center P.O. Box 273 Edwards, California 93523		1
Jet Propulsion Laboratory 4800 Oak Grove Drive Pasadena, California 91103		
Attention:	Library, Mail 111-113	1
NASA Manned Spacecraft Center 2101 Webster Seabrook Road Houston, Texas 77058		
Attention:	Library, Code BM6	1
NASA Marshall Space Flight Center Huntsville, Alabama 35812		
Attention:	Library	1
NASA Wallops Station Wallops Island, Virginia 23337		
Attention:	Library	1
NASA Electronics Research Center 575 Technology Square Cambridge, Massachusetts 02139		
Attention:	Library	1
NASA Lewis Research Center 21000 Brookpark Road Cleveland, Ohio 44135		
Attention:	Library, Mail Stop 60-3	1

SHEET

US 4802 1434 REV. 8-65

DISTRIBUTION LIST

NAS1-7954

	Copies each
NASA Goddard Space Flight Center Greenbelt, Maryland 20771 Attention: Library	1
NASA John F. Kennedy Space Center Kennedy Space Center, Florida 32899 Attention: Library, Code IS-CAS-42B	1
National Aeronautics and Space Administration Washington, D. C. 20546 Attention: Library, Code USS-10	1
L. Kosofsky, Code MAL	1
NASA Manned Spacecraft Center 2101 Webster Seabrook Raod Houston, Texas 77058 Attention: J. Sasser, Code TH3	3
W. R. Wollenhaupt, Code FM4	1
Army Map Service 6500 Brooks Lane Washington, D. C. 20315 Attention: D. Light, Code 12440	1
C. MacAfoos, Code 11910	1
Aeronautical Chart and Information Center 2nd and Arsenal Street St. Louis, Missouri 63118 Attention: C. F. Martin, ACDEG-2	1
R. Carder, ACO	1
National Space Science Data Cenyer Goddard Space Flight Center Greenbelt, Maryland 20771 Attention: K. Michlovitz, Code 601	50 plus reproducibles
Bellcomm, Inc. 995 L'Enfant Plaza North S.W. Washington, D. C. 20024 Attention: D. B. James	1
U. S. Geological Survey 345 Middlefield Road Menlo Park, California 94025 Attention: H. Masursky	2

USE FOR TYPEWRITTEN MATERIAL ONLY

SHEET

USE FOR TYPEWRITTEN MATERIAL ONLY

DISTRIBUTION LIST

NAS1-7954

	Copies each
Dr. Donald Wise Department Department of Geology Franklin Marshall College Lancaster, Pennsylvania 17604	1
University of Arizona Tucson, Arizona 85721 Attention: Dr. G. P. Kuiper	1
Professor E. A. Whitaker	1
University of California P. O. Box 109 LaJolla, California 92037 Attention: Dr. H. C. Urey	1
NASA Scientific and Technical Information Facility P. O. Box 33 College Park, Maryland 20740	17